

Manufacturing Letters

Manufacturing Letters 00 (2022) 000-000



50th SME North American Manufacturing Research Conference (NAMRC 50, 2022)

Generative Modeling of the Shape Transformation Capability of Machining Processes

Xiaoliang Yan^a, Shreyes Melkote^{a,*}

"George W. Woodruff School of Mechanical Engineering, Georgia Institute of Technology, Atlanta, Georgia, 30332

* Corresponding author. Tel.: +1-404-894-8499; fax: +1-404-894-9342. E-mail address: shreyes.melkote@me.gatech.edu

Abstract

The shape, material property, and part quality transformation capabilities of a manufacturing process are essential process capability knowledge that are traditionally acquired by process planners through experience. While efforts have been made over the years to develop automated systems that utilize known process capabilities for process selection and manufacturability assessment of part designs, such systems are hampered by the lack of a systematic approach to capture and model the shape, material property, and part quality transformation capabilities from design and manufacturing data. In this paper, the *shape transformation* capabilities of representative machining operations are modeled using 3D Variational Autoencoders and Generative Adversarial Networks (3D-VAE-GANs.) The proposed approach models the shape transformation capability as a latent probability distribution from which visualizations of realistic machinable features can be sampled for shape decomposition and reconstruction, thereby assisting machining process selection by a process planner and manufacturability assessment of part shapes generated by a designer.

© 2022 Society of Manufacturing Engineers (SME). Published by Elsevier Ltd. All rights reserved. This is an open access article under the CC BY-NC-ND license (http://creativecommons.org/licenses/by-nc-nd/4.0/) Peer-review under responsibility of the Scientific Committee of the NAMRI/SME.

Keywords: Generative Machine Learning; Machining Process Capability; Computer Aided Process Planning; Machining Feature Recognition

1. Introduction

In today's concurrent engineering environment, the emphasis is on seamless interaction between product designers and process planners to enable *manufacturability assessment of the design* and *process/operation selection* [1]. Traditionally, a process planner studies the part drawing and manufacturing specifications to recall and visualize similar parts or features from experience to identify the processes that can produce the desired part. This practice usually requires the process planner to be knowledgeable about the *process capability* of a manufacturing process defined in terms of its shape, material property, and part quality transformation capabilities [2]. Here, we define the shape transformation capability of a manufacturing process as the various shapes and features it can produce.

Efforts have been made to model the manufacturing process capability knowledge to assist process planners with key process related decisions [3]. Prior work on manufacturing process capability knowledge representation generally falls into two categories [4]. One, high-level descriptions of manufacturing resources (e.g. available machines [5] and labor skills [6]) are used to describe the process capability. Two, detailed descriptions are used to link manufacturing processes to part design attributes [7, 8]. A line of work is focused on shape information representation through Feature Recognition (FR) [9]. Prior researchers have implemented FR techniques such as syntactic pattern recognition [10], graph theory [11], hint-based recognition [12], expert systems [13], and neural networks [14]. However, traditional FR systems, e.g. graphbased systems, have limited capability for manufacturability assessment and process selection [15]. Ip and Regli [16] used a Support Vector Machine to discriminate between cast and



Figure 1. Machining process capability modeling for assessing manufacturability assessment of designs and for process/operation selection in process planning.

machined parts based on shape curvature distributions obtained from 3D CAD models. Hoefer and Frank [17] utilized part geometry metrics to extract key features that set manufacturing process constraints and subsequently trained process selection models using K-nearest-neighbor, decision trees and random forest classification methods. Zhao et al. [18] utilized decision trees to discriminate between the process capabilities of three manufacturing processes (casting, turning, milling) in terms of their part shape, material property, and quality attributes. These approaches, however, require selecting and preparing the data attributes as the first step.

Recent advances in 3-dimensional (3D) machine learning have rekindled interest in manufacturability assessment of design and process selection using 3D data-driven methods. Zhang et al. [19] presented FeatureNet for machining FR based on a 3D convolutional neural network (3D-CNN). Ghadai et al. [20] developed a framework for localized feature identification in manufacturability analysis of drilled holes. Peddireddy et al. [21] proposed a machining process identification system based on transfer learning from a trained 3D-CNN FR source model. While an increasing emphasis has been placed on bridging the gap between FR and manufacturability analysis and process selection, current state-of-the-art 3D data-driven methods suffer from limitations of discriminative neural networks, which perform classification in an implicit manner [2]. Importantly, a part can have a complex combination of features that must be machined by multiple processes using a sequence of operations. This multi-label classification task requires a large number of training classes consisting of combinations of machinable and non-machinable features of given processes/operations. Although algorithms developed for feature separation, labeling, and segmentation [19], the computational complexity renders discriminative classification models impractical for analyzing complex part designs and identifying sequences of processes.

An alternative 3D machine learning approach has been employed in design optimization. For instance, in design topology optimization, the intensive computational cost of Finite Element Analysis has led to research efforts that utilize deep generative models such as Variational Auto-Encoder (VAE) and Generative Adversarial Network (GAN) to generate near-optimal topological designs [22]. Banga et al. [23] employed a 3D encoder-decoder pair to optimize the design structure. Oh et al. [22] proposed a GAN-based topology

optimization framework, which was applied to 2D wheel design generation. Greminger [24] presented a 3D-GAN that enforces manufacturing constraints on topology optimization by training with known shapes manufactured by a 3-axis milling machine. While the above works have demonstrated the ability to impose and visualize topology constraints on design, few have emphasized manufacturability analysis, not to mention process and operation selection considerations.

It is evident that state-of-the-art 3D machine learning methods applied to FR are limited by the computational bottleneck arising from the multi-label nature of the problem, and generative design approaches, for the most part, lack manufacturability assessment and process considerations. For machining, a significant knowledge gap still exists between a part design and a process plan capable of transforming the design into a finished part owing to the lack of a method for automatically capturing process capability knowledge that can be utilized to map a part design to a manufacturing process. Recalling that a human process planner has implicit understanding of machining process capability that is usually acquired from experience, we hypothesize that the required machining process capability knowledge can be automatically learned through 3D data-driven generative machine learning methods.

As shown in Figure 1, we envision a "process capability advisor" powered by generative models of machining process capabilities that not only assist the designer with manufacturability assessment of part designs, but also facilitate process selection, which is a key step in process planning. The benefit of using the process capability advisor for process planning is to ensure that there is a scalable AI reference for validating process selection decisions, which currently rely on the individual experiential knowledge of process planners. In this paper, we limit our focus to generative modeling of the shape transformation capability of a machining process. The shape transformation capability is characterized by the shapes and spatial features that a process or an operation can produce. Specifically, we build on recent advances in generative machine learning models of 3D objects made by the machine vision and generative design communities to answer the following questions: (1) Can we learn the shape transformation capability of a machining process as a latent probability distribution using generative machine learning methods? and (2) How can the learned shape transformation capability be

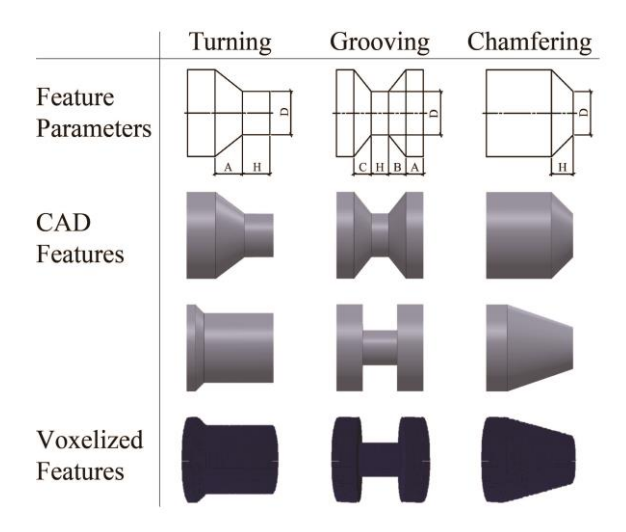


Figure 2. Data generation flow.

used for design manufacturability assessment and process selection? These questions are answered by developing and evaluating the performance of a combined 3D VAE and GAN generative modeling approach that can learn the shape transformation capability of typical shaping operations carried out on a lathe. The paper also shows how these generative models can be used for design manufacturability assessment and process/operation selection by providing automated *visual* feedback to designers and process planners, respectively. The shape transformation capability of a machining operation is learned as a latent probability distribution by fitting a high-dimensional multi-modal probability distribution to voxelized CAD models of part shapes during training of deep neural networks, from which we can sample easily interpretable 3D visualizations of shapes the machining operation can produce.

2. Data Generation

While numerous 3D machine learning datasets have been developed for training convolutional neural networks, curated 3D datasets for manufacturing are scarce. For this work, we synthesized three datasets consisting of parts machinable by turning, grooving, and chamfering operations that can be carried out on a lathe. Figure 2 shows the data generation flow, which follows the basic feature generation approach described by Peddireddy et al. [21]. The starting geometry of parts in all three datasets was a solid cylinder with diameter d. Each part was parameterized using feature size and feature position denoted by (C, H, B, A, D). The parameters were varied according to a uniform distribution and a pre-defined minimum allowable wall thickness. In this paper we set d to 100 mm and the minimum allowable wall thickness to 10 mm. One hundred and fifty models were generated for each machining operation. The CAD models were generated automatically using a Solidworks macro. The CAD models were subsequently converted into a voxelized representation with a resolution of $64 \times 64 \times 64$ using binvox [25], an open-source voxelizer library.

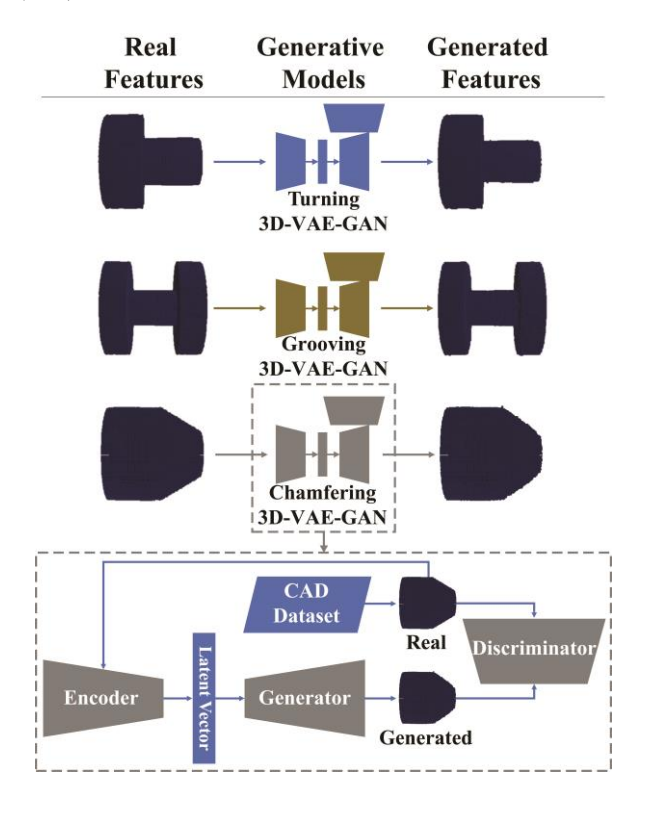


Figure 3. Overview of modeling approach.

3. Generative Modeling Approach

A distinction must be made between the discriminative modeling approach previously utilized in FR and MPI work and generative modeling. A discriminative model learns a conditional probability P(y|X) from a training dataset, where, in the context of machining, X are the data points, such as voxelized CAD models, and y are the corresponding labels, such as the machining process/operation label. In contrast, a generative model learns a joint probability P(X, y) from the dataset or P(X) if labels are not available. Sampling from the learned joint probability distribution generates a synthetic object of the same class as the training dataset. Wu et al. [26] presented a 3D Generative Adversarial Network (3D GAN) that learns a latent probability distribution to generate 3D objects. Shu et al. [27] employed a GAN using point cloud representations of aircraft to synthesize new designs. Dai et al. [28] developed a method to complete a partial 3D scan using a 3D Encoder-Predictor network. Li et al. [29] presented a method for structure-aware shape synthesis by generating parts using a combination of VAEs and GANs (VAE-GANs).

Considering the above, in this paper we employ a 3D-VAE-GAN framework to learn the shape transformation capability of a machining process exemplified by turning, grooving, and chamfering operations performed on a lathe. As shown in Figure 3, each 3D-VAE-GAN was trained on a dataset for a given operation. Neural networks with roles of "encoder," "generator," and "discriminator" were trained simultaneously. The encoder takes voxelized ground truth shapes from the dataset as inputs to learn a latent probability distribution of the shape transformation capability, while the generator generates realistic features that can be produced by the machining

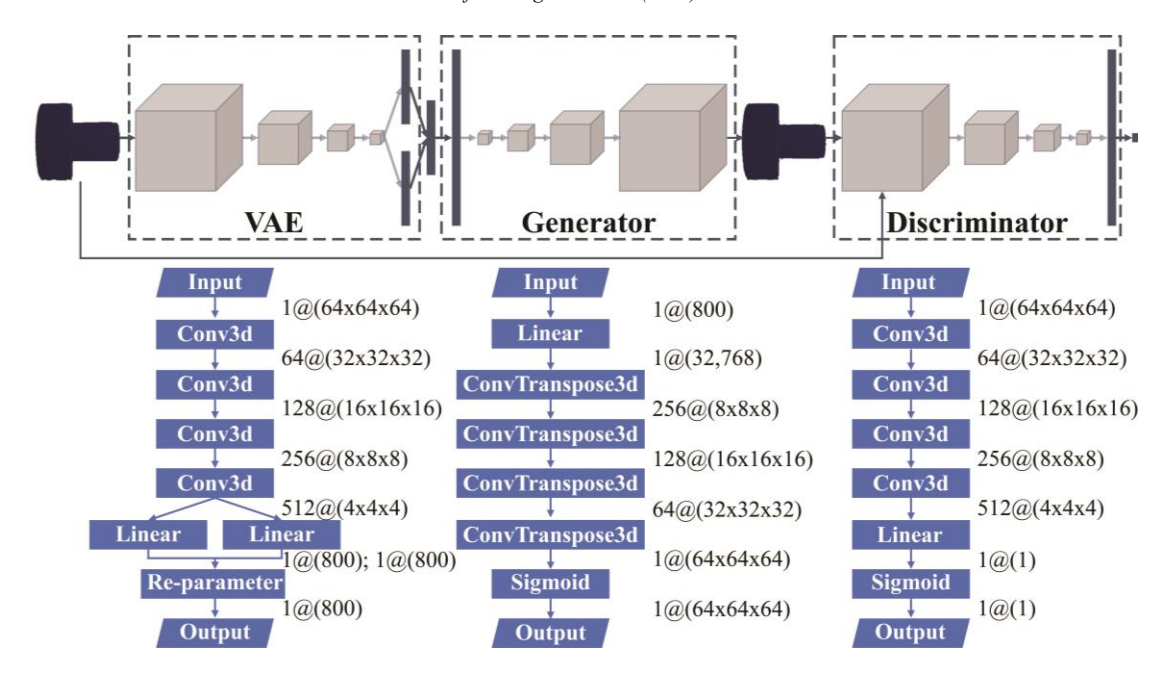


Figure 4. 3D-VAE-GAN architecture.

operation, and the discriminator judges the "fakeness" of the generator outputs.

3.1. Model Architecture

The architecture of the 3D-VAE-GAN used in this paper follows work reported in the literature on generative modeling of generic 3D objects [26, 30], and is shown in Figure 4. The VAE has four 3D-convolutional (Conv3d) layers and two linear layers. Batch normalization [31] and leaky rectified linear unit (LReLU) activation function [32] are applied after each Conv3d layer. LReLU is a non-linear activation function given by $LReLU(x) = \max(x, \alpha x)$, where α in this work is set to 0.2. The two fully connected linear layers following the Conv3d layers have dimensions of 800×1 with one vector designated as the mean vector and the other as the standard deviation vector of the latent probability distribution. Finally, a single 800×1 latent vector is obtained by sampling values from the mean and standard deviation vectors, which assumes the latent vector elements follow normal distributions. In the generator, a fully connected layer expands the dimension to $32,768 \times 1$ and is followed by four 3D-transpose-convolutional (ConvTranspose3d) layers. A sigmoid layer, which has the form of $S(x) = (1 + e^{-x})^{-1}$, is applied at the end to enforce a value between 0 and 1 for each voxel in the $64 \times 64 \times 64$ output. This output, along with the input to the VAE, are input to the discriminator. The discriminator has a network structure like that of the VAE, except for the linear layer which has an output dimension of 1. Again, a sigmoid layer is applied to output a probability of the input being fake.

3.2. Objective Functions

In a typical VAE encoder and decoder (generator) pair, the loss function for both networks is defined as follows:

$$\alpha_1 \|\hat{x} - x\|_2 + \alpha_2 KL[N(\mu, \Sigma) \|N(0, I)]$$

$$\tag{1}$$

where x is the input to the encoder, \hat{x} is the output of the generator, μ and Σ are the means and variances of the outputs produced by the encoder, and α_1 and α_2 are tuning parameters. The first term in the loss function returns the reconstruction loss from the encoder-generator pair, whereas the second term returns the Kullback-Leibler (KL) divergence of the latent vectors from a unit normal distribution. In this work, α_1 was set to 150, and α_2 was set to 2 to emphasize the reconstruction loss. In a 3D-VAE-GAN, an additional term based on the discriminator output is added to the generator loss function defined in Eq. (1) as follows:

$$\alpha_1 \| \hat{x} - x \|_2 + \alpha_2 KL[N(\mu, \Sigma) \| N(0, I)] + D(\hat{x})$$
 (2)

where $D(\hat{x})$ is the discriminator output that judges the fakeness of the generator output, \hat{x} .

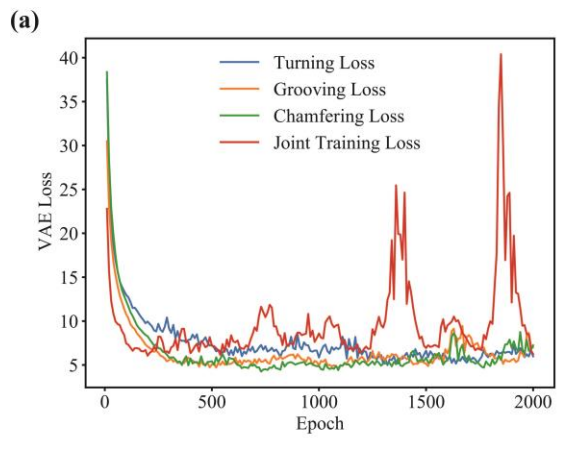
Note that the discriminator loss function in the original GAN [33] is defined as a minimax value function V(D, G):

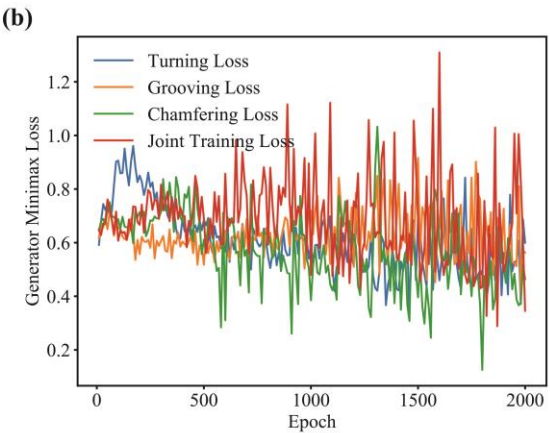
$$\min_{G} \max_{D} V(D, G) = \mathbb{E}_{x \sim P_{data}} \left[\log D(x) \right] + \mathbb{E}_{x \sim P_{noise}} \left[\log (1 - D(G(z))) \right]$$
(3)

However, the game-theory based loss function in Eq. (3) can lead to unstable training and mode collapse. We therefore employed the discriminator loss function used in the Improved Wasserstein GAN training system (IWGAN) [34], which has demonstrated superior results for 3D object reconstruction [30]:

$$\mathbf{E}_{\hat{x} \sim P_g} \left[D(\hat{x}) \right] - \mathbf{E}_{x \sim P_r} \left[D(x) \right] + \alpha_3 \mathbf{E}_{\hat{x} \sim P_x} \left[(|| \nabla_{\hat{x}} D(\hat{x}) ||_2 - 1)^2 \right]$$
(4)

where P_g and P_r are the generator and target distributions, respectively, P_x is the distribution sampled uniformly on a straight line between P_g and P_r , and the last term of the loss function is the gradient penalty that penalizes the deviation of





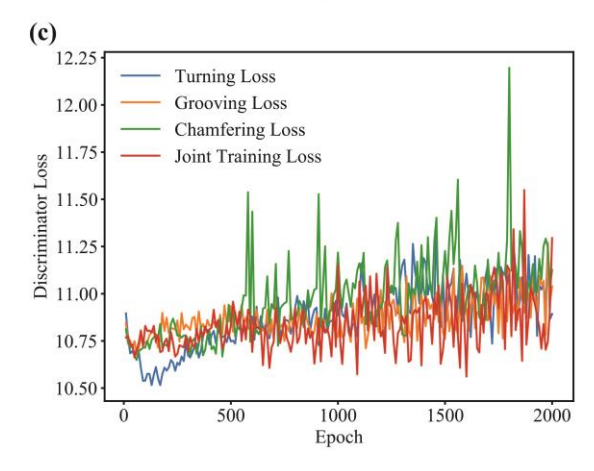


Figure 5. Training losses of (a) VAE, (b) generator minimax component, and (c) discriminator.

the discriminator's gradient from unity. The value of α_3 in this work was set to 10.

3.3. Model Training Approach

In this work, we trained a separate 3D-VAE-GAN model for each CAD dataset containing the shapes manufacturable by a given machining operation, which resulted in three 3D-VAE-GAN models, one for each machining operation. In addition to training 3D-VAE-GANs for the individual machining operations, a joint 3D-VAE-GAN was trained on a combined turning, grooving and chamfering dataset consisting of 450 parts for comparison. The models were constructed and trained using PyTorch [35], which is a deep learning library for Python.

(a)	Input	Turning Model	Joint Model
Object 1			2
Object 2			
Object 3			
Object 4			
Object 5			H
(b)	Input	Grooving Model	Joint Model
Object 1		94	
Object 2	H		H
Object 3			
Object 4		00	
Object 5		90	
(c)	Input	Chamfering Model	Joint Model
Object 1			
Object 2			
Object 3			
Object 4			
Object 5			

Figure 6. Shape generation comparison of the (a) turning model, (b) grooving model, and (c) chamfering model against the joint model.

Model training was performed on a high-performance computing node at the Georgia Institute of Technology (PACE Phoenix Cluster with 2 parallel NVIDIA Tesla V100 32GB GPUs). All three components of the 3D-VAE-GAN, namely the VAE, and discriminator, generator, were simultaneously on the training dataset for a given machining operation. For training all 3D-VAE-GANs, the batch size was set to 30. Adaptive moment estimation (Adam) [36] was used as the optimizer with initial exponential decay rates of the first and second moments of gradient, β_1 and β_2 , set to 0.8 and 0.99, respectively. The VAE and generator learning rates were set to 4×10^{-6} , and the discriminator learning rate was set to 2×10^{-6} . Note that these hyperparameters were manually tuned based on

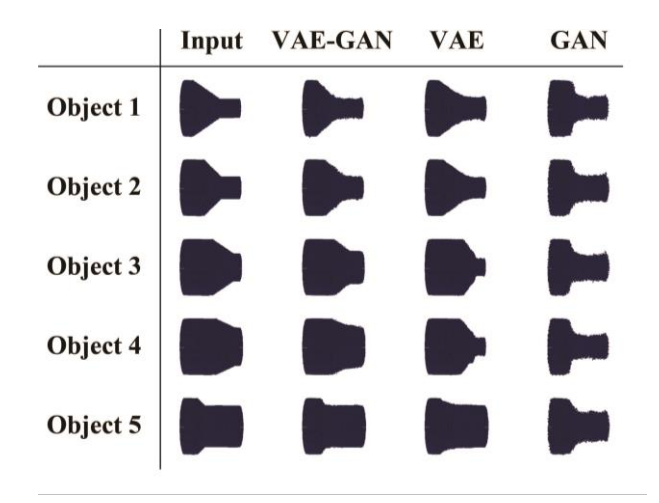


Figure 7. Shape generation comparison of VAE-GAN, VAE-Only, and GAN-Only models.

the training losses and visualization results of the 3D-VAE-GANs. It is expected that the hyperparameters will need to be re-tuned to optimize the performance for different training datasets. All 3D-VAE-GANs were trained for 2000 epochs.

4. Model Evaluation

As noted above, three models were trained, one for each machining operation, using their respective training datasets, and a joint model was trained using the combined dataset for all three operations. The purpose of training the joint model was to determine if training jointly is as effective as training separately on an individual operation dataset for learning the shape transformation capability of the operations.

The trained models were evaluated by observing the training losses and the shape transformation (3D object generation) results. Figure 5 shows the VAE loss given by Eq. (1), the minimax component of the generator loss $D(\hat{x})$, and the discriminator loss given by Eq. (4). Both the generator minimax loss and the discriminator loss demonstrated higher volatility as training progressed, which is expected as both the generator and the discriminator gradually improve through the adversarial training process, and the output probability of the discriminator approaches either 0 or 1. Although theoretical convergence does not exist in adversarial training, it can be seen from Figure 5 that the mean generator loss decreased, whereas the mean discriminator loss increased in the long run. The hyperparameters were purposely tuned to allow the generator to learn faster and eventually defeat the discriminator. It is also evident that the VAE losses decreased steadily for the turning, grooving and chamfering models before converging. However, the joint training model suffered from an instability in the VAE loss as the training epochs increased. Upon further investigation, the instability of the VAE loss for the joint model was attributed to a significant KL divergence, which indicates that the structure of the latent probability distribution was not effectively embedded through learning from the combined dataset using the same hyperparameters used for the individually trained models.

In addition to the training losses, training data reconstructions were visualized as shown in Figure 6 to

evaluate the effectiveness of the learned shape transformation capability. The inputs to the trained models were randomly selected from the training dataset. It is evident from the three sub-figures that the outputs of the separately trained models and the joint model capture the shapes of the corresponding input objects, confirming that the generative modeling approach used in this paper is able to capture the shape transformation capability as a latent probability distribution. However, the joint model is unable to generate objects with the same details and clarity as the individual operation models. This observation reflects the significantly higher VAE loss of the joint model in Figure 5, as the difficulty in simultaneously learning the latent probability distribution of all three operations was higher than training individual models for each operation.

Based on the training loss and visualization comparisons, it is evident that models for the individual operations outperform the joint model in capturing the shape transformation capability of the machining operations considered. Note that this result aligns with the reported precision score for a nonmanufacturing dataset (IKEA 2D image to 3D object dataset) [30, 37], where separately trained models consistently outperformed jointly trained models. This suggests that instead of treating a deep generative model such as a 3D-VAE-GAN as a "black box," an emphasis must be placed on creating training datasets with intrinsic characteristics based on machining domain knowledge to reduce learning difficulty. For example, a machining dataset can be organized as a hierarchy of starting geometries, machining processes, and operations, from which the hierarchical level of training data determines the learning difficulty.

To illustrate the superior performance of the 3D-VAE-GAN architecture for modeling the shape transformation capability, two additional deep generative modeling architectures, namely VAE-only and GAN-only models, were constructed and trained using the same hyperparameters listed above. Figure 7 shows the shape generation results of the three deep generative architectures for the same inputs. The GAN-only architecture produced the worst results due to mode-collapse i.e. generating only a handful of shapes without learning an accurate latent probability distribution. The VAE-only approach resulted in shapes like those produced by the 3D-VAE-GAN, which indicates that a more accurate latent probability distribution is learned. However, rounded edges are more prevalent due to the lack of a discriminator. Similar results have been reported in the computer vision literature [38], where blurry images are observed. It is evident that the VAE-GAN architecture combines the benefits of both VAE and GAN architectures to produce the best overall results.

The foregoing results suggest that, with an optimized dataset, model architecture and training hyperparameters, the shape transformation capability of a machining process can be captured sufficiently well for shape decomposition and reconstruction.

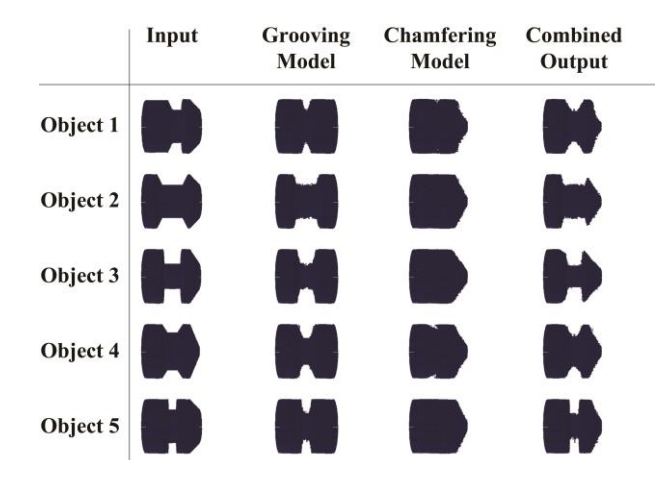


Figure 8. Successful design decomposition and reconstruction.

	Input	Grooving Model	Turning Model	Combined Output
Object 1	H			
Object 2				
Object 3	H	H		
Object 4				
Object 5				

Figure 9. Unsuccessful design decomposition and reconstruction.

5. Shape Decomposition and Reconstruction

In the previous section, we demonstrated the ability to learn the shape transformation capability of a machining process using a generative machine learning approach. The next question is: how can the learned shape transformation capability be utilized for design manufacturability assessment and process/operation selection? An example use case is shape decomposition and reconstruction. Contrary to discriminative models that yield a probability as output, our shape transformation capability models are capable of decomposing and visualizing a part design as machinable features, which enable the part designer to evaluate manufacturability of the design using the selected process/operation.

A unique property of VAE-based generative models is their ability to compensate for missing information in the input, which has been demonstrated for 3D scan shape completion [28], and 3D shape generation from 2D images [26]. Considering that machining is a material removal process, our shape transformation capability models were trained such that only features that are machinable by the selected operation are output. When the output sampled from the latent probability distribution of a 3D-VAE-GAN matches the input shape, it implies that the input is drawn from the latent probability distribution and can therefore be produced by the

process/operation. Conversely, if the output sampled from the latent probability distribution does not match the input, the implication is that the input shape cannot be produced by the process/operation. Therefore, by comparing the reconstructed input shape to the output shape, the manufacturability of the input shape by the machining operation can be determined. In Figure 8 and Figure 9, the query 3D objects are input to all VAE-GAN models, which return outputs sampled from the generative capability models of the respective machining operations. The combined outputs are obtained from an intersection Boolean operation (in the voxel space) of the generative model outputs. Figure 8 shows an example of a successful decomposition of an unseen input part shape into features that can be machined by the different operations. In this case, the inputs contain both a groove and a chamfer. The shape transformation capability models did not observe such feature combinations during training, but the grooving model returned a shape with a groove, which closely resembles the input, while the chamfering model only returned a chamfer. By reconstructing a combined object from the outputs of the grooving and chamfering models through an intersection Boolean operation, the result yields a visualization of a part closely matching the input shape. Figure 9 shows examples of unsuccessful decompositions and reconstructions. While the grooving model returned a decomposed groove feature, the turning model could only return the closest matching turning feature and not a chamfer. As a result, the reconstructed objects in Figure 9 do not resemble the inputs. By visually comparing the reconstructed output with the input, a designer can determine the manufacturability of the design by the available process/process combination while a process planner can identify a viable process/process combination to produce the shapes contained in the design.

6. Conclusion

In this paper we proposed a deep generative machine learning approach to learn the shape transformation capability of representative machining operations. By modeling the shape transformation capabilities of turning, grooving and chamfering operations using 3D-VAE-GANs, we demonstrated that (1) the shape transformation capability of a machining process can be learned as a latent probability distribution, (2) visualization of machinable features can be obtained by sampling from the shape transformation capability model, (3) separately trained models can capture the shape transformation capability of a machining operation better than a jointly trained model, which indicates that domain knowledge should be used to create datasets that minimize learning difficulty, and (4) the learned shape transformation capability can be used for shape decomposition and reconstruction, through which manufacturability of the part design can be visualized and a suitable machining process/operation can be selected. By enabling explainable process decisions through visualization, the generative modeling of machining process capability can enable design for manufacturing and accelerated process planning.

There are of course limitations to the models presented herein, which will be addressed in future work. Specifically, the robustness of the models can be improved by considering the dimensions, positions, and tolerances of a feature. Another extension is to include other machining processes/operations in the model. Finally, material and part quality transformation capabilities need to be integrated with shape transformation for more accurate representation of the machining process capability.

Acknowledgements

This work was funded by an EAGER grant from the National Science Foundation (Award # 2113672).

References

- [1] G. Halevi and R. Weill, *Principles of process planning: a logical approach*. Springer Science & Business Media, 1994.
- [2] M. Al-wswasi, A. Ivanov, and H. Makatsoris, "A survey on smart automated computer-aided process planning (ACAPP) techniques," *The International Journal of Advanced Manufacturing Technology*, vol. 97, no. 1, pp. 809-832, 2018.
- [3] J. Shah, P. Sreevalsan, and A. Mathew, "Survey of CAD/feature-based process planning and NC programming techniques," *Computer-Aided Engineering Journal*, vol. 8, no. 1, pp. 25-33, 1991.
- [4] M. E. A. Algeo, "A state-of-the-art survey of methodologies for representing manufacturing process capabilities," *NIST Report NISTIR*, vol. 5391, 1994.
- [5] H.-M. Xu and D.-B. Li, "A clustering-based modeling scheme of the manufacturing resources for process planning," *The International Journal of Advanced Manufacturing Technology*, vol. 38, no. 1-2, p. 154, 2008.
- [6] S. C. Feng and E. Y. Song, "A manufacturing process information model for design and process planning integration," *Journal of Manufacturing Systems*, vol. 22, no. 1, pp. 1-15, 2003.
- [7] S. Nelaturi, W. Kim, and T. Kurtoglu, "Manufacturability feedback and model correction for additive manufacturing," *Journal of Manufacturing Science and Engineering*, vol. 137, no. 2, 2015.
- [8] D. Šormaz, M. Wakh, and N. Arafat, "Rule-based process planning and setup planning with considerations of Gd & T requirements," *Int J* "Advanced Quality, vol. 45, no. 1, pp. 13-20, 2017.
- [9] S. Joshi and T.-C. Chang, "Feature extraction and feature based design approaches in the development of design interface for process planning," *Journal of Intelligent Manufacturing*, vol. 1, no. 1, pp. 1-15, 1990.
- [10] B. Prabhu and S. Pande, "Intelligent interpretation of CADD drawings," *Computers & Graphics*, vol. 23, no. 1, pp. 25-44, 1999.
- [11] S. Chuang and M. R. Henderson, "Three-dimensional shape pattern recognition using vertex classification and vertex-edge graphs," *Computer-Aided Design*, vol. 22, no. 6, pp. 377-387, 1990.

- [12] A. Verma and S. Rajotia, "A hint-based machining feature recognition system for 2.5 D parts," *International journal of production research*, vol. 46, no. 6, pp. 1515-1537, 2008.
- [13] P. K. Venuvinod and S. Wong, "A graph-based expert system approach to geometric feature recognition," *Journal of Intelligent Manufacturing*, vol. 6, no. 3, pp. 155-162, 1995.
- [14] M. Korosec, J. Balic, and J. Kopac, "Neural network based manufacturability evaluation of free form machining," *International Journal of Machine Tools and Manufacture*, vol. 45, no. 1, pp. 13-20, 2005.
- [15] A. K. Verma and S. Rajotia, "A review of machining feature recognition methodologies," *International Journal of Computer Integrated Manufacturing*, vol. 23, no. 4, pp. 353-368, 2010.
- [16] C. Y. Ip and W. C. Regli, "A 3D object classifier for discriminating manufacturing processes," *Computers & Graphics*, vol. 30, no. 6, pp. 903-916, 2006.
- [17] M. J. Hoefer and M. C. Frank, "Automated manufacturing process selection during conceptual design," *Journal of Mechanical Design*, vol. 140, no. 3, 2018.
- [18] C. Zhao, M. Dinar, and S. N. Melkote, "Automated classification of manufacturing process capability utilizing part shape, material, and quality attributes," *Journal of Computing and Information Science in Engineering*, vol. 20, no. 2, p. 021011, 2020.
- [19] Z. Zhang, P. Jaiswal, and R. Rai, "Featurenet: Machining feature recognition based on 3d convolution neural network," *Computer-Aided Design*, vol. 101, pp. 12-22, 2018.
- [20] S. Ghadai, A. Balu, S. Sarkar, and A. Krishnamurthy, "Learning localized features in 3D CAD models for manufacturability analysis of drilled holes," *Computer Aided Geometric Design*, vol. 62, pp. 263-275, 2018.
- [21] D. Peddireddy *et al.*, "Identifying manufacturability and machining processes using deep 3D convolutional networks," *Journal of Manufacturing Processes*, vol. 64, pp. 1336-1348, 2021.
- [22] S. Oh, Y. Jung, S. Kim, I. Lee, and N. Kang, "Deep generative design: Integration of topology optimization and generative models," *Journal of Mechanical Design*, vol. 141, no. 11, 2019.
- [23] S. Banga, H. Gehani, S. Bhilare, S. Patel, and L. Kara, "3d topology optimization using convolutional neural networks," *arXiv preprint arXiv:1808.07440*, 2018.
- [24] M. Greminger, "Generative Adversarial Networks With Synthetic Training Data for Enforcing Manufacturing Constraints on Topology Optimization," in *International Design Engineering Technical Conferences and Computers and Information in Engineering Conference*, 2020, vol. 84003, p. V11AT11A005: American Society of Mechanical Engineers.
- [25] P. Min, "binvox," ed, 2004-2021.
- [26] J. Wu, C. Zhang, T. Xue, W. T. Freeman, and J. B. Tenenbaum, "Learning a probabilistic latent space of object shapes via 3d generative-adversarial

- modeling," in *Proceedings of the 30th International Conference on Neural Information Processing Systems*, 2016, pp. 82-90.
- [27] D. Shu *et al.*, "3d design using generative adversarial networks and physics-based validation," *Journal of Mechanical Design*, vol. 142, no. 7, p. 071701, 2020.
- [28] A. Dai, C. Ruizhongtai Qi, and M. Nießner, "Shape completion using 3d-encoder-predictor cnns and shape synthesis," in *Proceedings of the IEEE Conference on Computer Vision and Pattern Recognition*, 2017, pp. 5868-5877.
- [29] J. Li, C. Niu, and K. Xu, "Learning part generation and assembly for structure-aware shape synthesis," in *Proceedings of the AAAI Conference on Artificial Intelligence*, 2020, vol. 34, no. 07, pp. 11362-11369.
- [30] E. J. Smith and D. Meger, "Improved adversarial systems for 3d object generation and reconstruction," in *Conference on Robot Learning*, 2017, pp. 87-96: PMLR.
- [31] J. Bjorck, C. Gomes, B. Selman, and K. Q. Weinberger, "Understanding batch normalization," arXiv preprint arXiv:1806.02375, 2018.
- [32] B. Xu, N. Wang, T. Chen, and M. Li, "Empirical evaluation of rectified activations in convolutional network," *arXiv preprint arXiv:1505.00853*, 2015.

- [33] I. Goodfellow et al., "Generative adversarial nets," Advances in neural information processing systems, vol. 27, 2014.
- [34] I. Gulrajani, F. Ahmed, M. Arjovsky, V. Dumoulin, and A. Courville, "Improved training of wasserstein gans," *arXiv preprint arXiv:1704.00028*, 2017.
- [35] A. Paszke *et al.*, "Pytorch: An imperative style, high-performance deep learning library," *Advances in neural information processing systems*, vol. 32, pp. 8026-8037, 2019.
- [36] D. P. Kingma and J. Ba, "Adam: A method for stochastic optimization," *arXiv* preprint *arXiv*:1412.6980, 2014.
- [37] J. J. Lim, H. Pirsiavash, and A. Torralba, "Parsing ikea objects: Fine pose estimation," in *Proceedings of the IEEE International Conference on Computer Vision*, 2013, pp. 2992-2999.
- [38] J. Bao, D. Chen, F. Wen, H. Li, and G. Hua, "CVAE-GAN: fine-grained image generation through asymmetric training," in *Proceedings of the IEEE international conference on computer vision*, 2017, pp. 2745-2754.